J|A|C|S
ARTICLES
Published on Web 03/16/2006

Fine Tuning of the Rotary Motion by Structural Modification in Light-Driven Unidirectional Molecular Motors

Javier Vicario, Martin Walko, Auke Meetsma, and Ben L. Feringa*

Contribution from the Department of Organic and Molecular Inorganic Chemistry, Stratingh Institute, University of Groningen, Nijenborgh 4, 9747 AG, Groningen, The Netherlands

Received December 7, 2005; E-mail: b.l.feringa@rug.nl

Abstract: The introduction of bulky substituents at the stereogenic center of light-driven second-generation molecular motors results in an acceleration of the speed of rotation. This is due to a more strained structure with elongated C═C bonds and a higher energy level of the ground state relative to the transition state for the rate-limiting thermal isomerization step. Understanding the profound influence that variation of the substituent at the stereogenic center holds over the rotational speed of the light-driven molecular motor has enabled the development of the fastest molecular motor reported thus far.

Introduction

The design of nanodevices in which controlled motion at the molecular level can be achieved is essential for the development of the future toolbox of nanotechnology.[1] To power future nanomachines, new and faster molecular motors should be developed. Inspired by the fascinating molecular motors present in biological systems,[2] such as the kinase linear motor[3] and the ATP-ase rotary motor,[4] several synthetic motors have been designed,[5] in which controlled molecular motion is observed. Synthetic approaches toward artificial machinery have resulted in several elegant molecular systems in which an external stimulus induces controlled motion at the molecular level, including molecular propellers,[6] switches,[7] brakes,[8] turnstiles,[9] shuttles,[10] scissors,[11] elevators,[12] rotating modules,[13] muscles,[14] rotors,[15] ratchets,[16] and catalytic self-propelled objects.[17]

The first light-driven molecular motor **1** (Chart 1) was based on a sterically overcrowded symmetric biphenanthrylidene.[18] Key features of this motor are its intrinsic helical shape, the photoisomerizable C═C bond, and two stereogenic centers with a methyl substituent that, due to steric hindrance, adopts an energetically preferred pseudoaxial orientation. In this system, repetitive unidirectional rotation around the central double bond (the axis of rotation) is achieved by two energetically uphill photochemical steps each followed by an energetically downhill thermal step. Upon irradiation, cis/trans isomerization occurs with inversion of the helicity and simultaneous change in the conformation of the six-membered ring, forcing the methyl substituents to adopt a less favored pseudoequatorial orientation.

Chart 1. First Light-Driven Molecular Motor **1** and Second-Generation Molecular Motors **2** (One Enantiomer Shown)

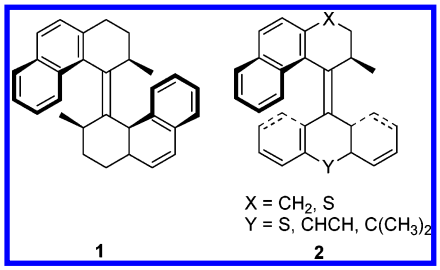

(1) (a) Nanotech: The Science of Small Gets Down to Business, Special Issue. *Sci. Am.* **2001**, *September*. (b) Feynmann R. P. In *Miniaturization*; Gilbert, H. D., Ed.; Reinhold: New York, 1961. (c) Balzani, V.; Venturi, M.; Credi, A. *Molecular Devices and Machines − A Journey into the Nanoworld*; Wiley-VCH: Weinheim, 2003.
(2) *Molecular Motors*; Schillwa, M., Ed.; Wiley-VCH: Weinheim, 2003.
(3) Vale, R. D.; Milligan, R. A. *Science* **2000**, *88*, 88.
(4) (a) Boyer, P. D. *Angew. Chem., Int. Ed.* **1998**, *37*, 2296. (b) Walker, J. E. *Angew. Chem., Int. Ed.* **1998**, *37*, 2308.
(5) (a) *Molecular Catenanes, Rotaxanes and Knots*; Sauvage, J.-P., Dietrich-Buchecker, C., Eds.; Wiley-VCH: Weinheim, 1999. (b) Balzani, V.; Gómez-López, M.; Stoddart, J. F. *Acc. Chem. Res.* **1998**, *31*, 405. (c) Stoddart, J. F., Ed. Molecular Machines, Special Issue. *Acc. Chem. Res.* **2000**, *100*, 409.
(6) Iwamura, H.; Mislow, K. *Acc. Chem. Res.* **1988**, *21*, 175.
(7) (a) Irie, M., Ed. Photochroism: Memories and Switches, Special Issue. *Chem. Rev.* **2000**, *100*, 1683. (b) *Molecular Switches*; Feringa, B. L., Ed.; Wiley-VCH: Weinheim, 2001.
(8) Kelly, T. R.; Bowyer, M. C.; Bhaskar, K. V.; Bebbington, D.; García, A.; Lang, F.; Kim, M. H.; Jette, M. P. *J. Am. Chem. Soc.* **1994**, *116*, 3657.
(9) Bedard, T. C.; Moore, J. S. *J. Am. Chem. Soc.* **1995**, *117*, 10662.
(10) (a) Ashton, P.; Baldoni, V. R.; Balzani, V.; Credi, A.; Hoffman, H. D. A.; Martínez-Díaz, M. V.; Raymo, F. M.; Stoddart, J. F.; Venturi, M. *Chem.-Eur. J.* **2001**, *7*, 3482. (b) Pease, A. R.; Jeppesen, J. O.; Stoddart, J. F.; Luo, Y.; Collier, C. P.; Heath, J. R. *Acc. Chem. Res.* **2001**, *34*, 433. (c) Ballardini, R.; Balzani, V.; Credi, A.; Gandolfi, M. T.; Venturi, M. *Acc. Chem. Res.* **2001**, *34*, 445. (d) Brower, A. M.; Frochot, T.; Gatti, F. G.; Leigh, D. A.; Mottier, L.; Paolucci, F.; Roffia, S.; Wurpel, G. W. H. *Science* **2001**, *291*, 2124. (e) Jiménez-Molero, M. C.; Dietrich-Buchecker, C.; Sauvage, J.-P. *Chem.-Eur. J.* **2002**, *8*, 1456. (f) Bottari, G.; Leigh, D. A.; Pérez, E. M. *J. Am. Chem. Soc.* **2003**, *125*, 13360. (g) Da Ros, T.; Guldi, D. M.; Farrán Morales, A.; Leigh, D. A.; Prato, M.; Turco, R. *Org. Lett.* **2003**, *5*, 689. (h) Chang, S.-Y.; Jeong, K.-S. *J. Org. Chem.* **2003**, *68*, 4041. (i) Altieri, A.; Gatti, F. G.; Kay, E. R.; Leigh, D. A.; Martel, D.; Paolucci, F.; Slawin, A. M. Z.; Wong, J. K. Y. *J. Am. Chem. Soc.* **2003**, *125*, 8644. (j) Huang, T. J.; Tseng, H.-R.; Sha, L.; Lu, V.; Brough, B.; Flood, A. H.; Yu, B.-D.; Celestre, P. C.; Chang, J. P.; Stoddart, J. F.; Ho, C.-M. *Nano Lett.* **2004**, *4*, 2065. (k) Keaveney, C. M.; Leigh, D. A. *Angew. Chem., Int. Ed.* **2004**, *43*, 1222. (l) Steuermann, D. W.; Tseng, H.-R.; Peters, A. J.; Flood, A. H.; Jeppesen, J. O.; Nielsen, K. A.; Stoddart, J. F.; Heath, J. R. *Angew. Chem., Int. Ed.* **2004**, *43*, 6486.
(11) Muraoka, T.; Kinbara, K.; Kobayashi, Y.; Aida, T. *J. Am. Chem. Soc.* **2003**, *125*, 5612.
(12) Badjiæ, J. D.; Balzani, V.; Credi, A.; Silvi, S.; Stoddart, J. F. *Science* **2004**, *303*, 1845.
(13) Tashiro, K.; Konishi, K.; Aida, T. *J. Am. Chem. Soc.* **2000**, *122*, 7921.
(14) Jiménez, M. C.; Dietrich-Buchecker, C.; Sauvage, J.-P. *Angew. Chem., Int. Ed.* **2000**, *39*, 3284.

Chart 2. Five-Membered Symmetric Molecular Motor **3**, Its Second-Generation Analogue **4**, and Molecular Motor **5** with Electronic Control of the Speed of Rotation (One Enantiomer Shown)

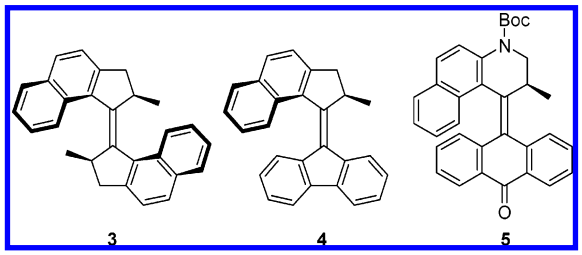

To revert to the most favored pseudoaxial conformation of the methyl substituents, the naphthalene upper part must slip past the lower part of the molecule, resulting in an irreversible thermal isomerization with simultaneous helix inversion. The energy barrier for this thermal isomerization is the main factor governing the speed of the overall rotary cycle. A significant disadvantage for further applications of this system is that a substantial amount of energy is required to overcome the barriers of the thermal helix inversion steps to induce a continuous rotary motion.

With the design of the second-generation molecular motors **2** (Chart 1), it was possible to reduce the energy barriers significantly by changing the bridging atoms X and Y.[19] A decrease of the size of X and Y reduces the steric hindrance in the "fjord region" of the molecule, decreasing the energy level of the transition state for the thermal step, which results in a lower Gibbs free energy of activation for the thermal helix inversion. Accordingly, the presence of smaller moieties X and Y results in faster thermal rotary steps in these motors. Consistent with these design features, molecular motor **3**[20] (Chart 2) in which the six-membered rings present in **1** were replaced by five-membered rings shows an increase in the speed of rotation due to the considerable reduction of the steric hindrance in the "fjord region". Recently, we reported the fast unidirectional light-driven molecular motor **4**[21] (Chart 2), which showed an increase of the speed of rotation by a factor of approximately 10^8 as compared to its six-membered ring upper half analogue, as well as an electronic control of the rotary speed due to a push−pull effect of the amino and carbonyl groups on the olefinic bond of molecular motor **5**.[22]

Chart 3. Molecular Motors with Reduced Size in the Arene Upper Half **6**, Displacement of the Methyl Substituent out of the "Fjord Region" **7**, and Different Size Substituents **8** (One Enantiomer Shown)

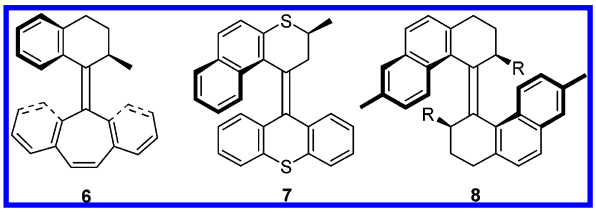

Surprisingly, the reduction in the size of the upper arene part of **6**[23] (Chart 3) or the displacement of the methyl substituent out of the "fjord region" in **7**[24] (Chart 3) resulted in an increase of the energy barriers and a reduction in the speed of rotation. This remarkable effect is attributed to a stabilization of the ground state of the unstable isomer of these molecules relative to the transition state, indicating that not only the steric hindrance in the "fjord region" but also conformational effects in the upper half are involved in governing the thermal isomerization process. The recent study of the thermal helix inversion process in first-generation six-membered molecular motors **8**[25] supports this multiple dependency on structural parameters (Chart 3).

The precise control over the rotary speed and the elucidation of the parameters governing the rotary motion is a major challenge in the design of future generations of molecular motors. The steric hindrance in the "fjord region" has a profound influence on the energy barriers for the thermal helix inversion; however, it is evident that the energy level of the ground state plays also a significant role. With this assumption, it is feasible to achieve further acceleration of light-driven molecular motors. This can be achieved by the reduction of the Gibbs free energy of activation of the thermal helix inversion step lowering the energy of the transition state through release of steric hindrance in the fjord region (Figure 1, case a), or by increasing the energy of the ground state, for instance, introducing larger substituents at the stereogenic center (Figure 1, case b).

Results and Discussion

On the basis of the observations summarized above, we anticipated that fine tuning of the speed of rotation of our recently reported fast light-driven molecular motor **4** might be achieved by introducing different size substituents at the stereogenic center, as shown for the new overcrowded alkenes **9a**−**c** (Chart 4).

Density functional theory (DFT) calculations were performed for the alkenes **4** and **9a**−**c** to determine the expected geometry

(15) (a) Schoevaars, A. M.; Kruizinga, W.; Zijlstra, R. W. J.; Veldman, L.; Spek, A. L.; Feringa, B. L. *J. Org. Chem.* **1997**, *62*, 4943. (b) Bermudez, V.; Capron, N.; Gase, T.; Gatti, F. G.; Kajzar, F.; Leigh, D. A.; Zerbetto, F.; Zhang, S. *Nature* **2000**, *406*, 608. (c) Domínguez, Z.; Dang, H.; Strouse, M. J.; García-Garibay, M. A. *J. Am. Chem. Soc.* **2002**, *124*, 2398. (d) Godlinez, C. E.; Zepada, G.; García-Garibay, M. A. *J. Am. Chem. Soc.* **2002**, *124*, 7719. (e) Domínguez, Z.; Dang, H.; Strouse, M. J.; García-Garibay, M. A. *J. Am. Chem. Soc.* **2002**, *124*, 8827. (f) Kuwatani, Y.; Yamamoto, G.; Iyoda, M. *Org. Lett.* **2003**, *5*, 3371. (g) Domínguez, Z.; Khuong, T.-A. V.; Dang, H.; Sanrame, C. N.; Núñez, J. E.; García-Garibay, M. A. *J. Am. Chem. Soc.* **2003**, *125*, 8827. (h) Leigh, D. A.; Wong, J. K. Y.; Dehez, F.; Zerbetto, F. *Nature* **2003**, *424*, 174. (i) Hawthorne, M. F.; Zink, J. I.; Skelton, J. M.; Bayer, M. J.; Liu, C.; Livshits, E.; Baer, R.; Neuhauser, D. *Science* **2004**, *303*, 1848. (j) Carella, A.; Rappenne, G.; Launey, J.-P. *New J. Chem.* **2005**, *29*, 288. (k) For a comprehensive review, see: Kottas, G. S.; Clarke, L. I.; Horinek, D.; Michl, J. *Chem. Rev.* **2005**, *105*, 1281.
(16) (a) Kelly, T. R.; Sestelo, J. P.; Tellitu, I. *J. Org. Chem.* **1998**, *63*, 3655. (b) Harrington, L. E.; Cahill, L. S.; McGlinchey, M. J. *Organometallics* **2004**, *23*, 2884.
(17) (a) Ismagilov, R. F.; Schwartz, A.; Bowden, N.; Whitesides, G. M. *Angew. Chem., Int. Ed.* **2002**, *41*, 652. (b) Paxton, W. F.; Kisler, K. C.; Olmeda, C. C.; Sen, A.; St. Angelo, S. K.; Coa, Y.; Mallouk, T. E.; Lammert P. E.; Crespi, V. H. *J. Am. Chem. Soc.* **2004**, *126*, 13424. (c) Catchmark, J. M.; Subramanian, S.; Sen, A. *Small* **2005**, *1*, 202. (d) Kline, T. R.; Paxton, W. F.; Mallouk, T. E.; Sen, A. *Angew. Chem., Int. Ed.* **2005**, *44*, 744. (e) Fournier-Bidoz, S.; Arsenault, A. C.; Manners, I.; Ozin, G. A. *Chem. Commun.* **2005**, 441. (f) Vicario, J.; Eelkema, R.; Browne, W. R.; Meetsma, A.; La Crois, R. M.; Feringa, B. L. *Chem. Commun.* **2005**, 3936.
(18) Koumura, N.; Zijlstra, R. W. J.; van Delden, R. A.; Harada, N.; Feringa, B. L. *Nature* **1999**, *401*, 152.
(19) Koumura, N.; Geertsema, E. M.; van Gelder, M. B.; Meetsma, A.; Feringa, B. L. *J. Am. Chem. Soc.* **2002**, *124*, 5037.
(20) ter Wiel, M. K. J.; van Delden, R. A.; Meetsma, A.; Feringa, B. L. *J. Am. Chem. Soc.* **2003**, *125*, 15076.
(21) Vicario, J.; Meetsma, J.; Feringa, B. L. *Chem. Commun.* **2005**, 5910.
(22) Pijper, D.; van Delden, R. A.; Meetsma, A.; Feringa, B. L. *J. Am. Chem. Soc.* **2005**, *127*, 17612.
(23) Geertsema, E. M.; Koumura, N.; ter Wiel, M. K. J.; Meetsma, A.; Feringa, B. L. *Chem. Commun.* **2002**, 2962.
(24) van Delden, R. A.; ter Wiel, M. K. J.; de Jong, H.; Meetsma, A.; Feringa, B. L. *Org. Biomol. Chem.* **2004**, *2*, 1531.
(25) ter Wiel, M. K. J.; van Delden, R. A.; Meetsma, A.; Feringa, B. L. *J. Am. Chem. Soc.* **2005**, *127*, 14208.

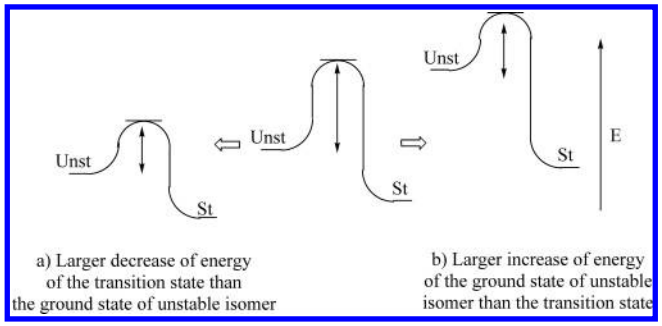

Figure 1. Energy diagrams showing possible modifications for the thermal helix inversion step. Unst = unstable isomer, St = stable isomer. Both unstable and stable isomers show a decrease (a) and an increase (b) in energy, respectively.

Chart 4. Proposed Structures of Alkenes **9** with Different Size Substituents at the Stereogenic Center

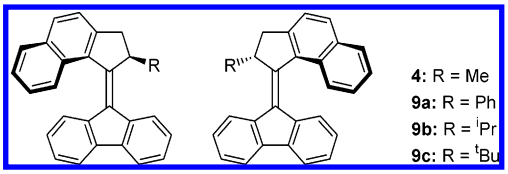

Table 1. Calculation of the Geometry for the Unstable Isomers and Energy Barriers of Alkenes **9** and **4**[a]

alkene	R	torsion angles (deg)	bond length (Å)	ΔG_{St-TS} (kJ mol^{-1})	$\Delta G_{Unst-TS}$ (kJ mol^{-1})
9a	Ph	28.89	1.3753	108.2	94.6
4	Me	30.45	1.3775	102.8	89.4
9b	^{i}Pr	31.58	1.3800	98.3	88.2
9c	^{t}Bu	38.22	1.3859	88.6	67.3

[a] St = stable isomer, Unst = unstable isomer, TS = transition state.

of the unstable forms, as well as the different energy barriers involved in the thermal isomerization processes (Table 1). From the calculated data, it is clear that by increasing the size of the substituent at the stereogenic center, the structure becomes more strained, as is indicated by the increase in torsion angles between the naphthalene upper half and fluorene lower half. The substituent seems to push the upper half out of the plane of the lower half, resulting in reduced "double bond character" in the central olefinic bond and increase in the C=C distance. As a consequence, the naphthalene upper half can slip past the lower half more easily during helix inversion. In principle, a Ph substituent is supposed to be larger than a Me group, but the planarity present in the aryl group allows a less strained structure due to a parallel conformation relative to the fluorene lower half. From the DFT energy optimization of the unstable isomers of alkenes **4** and **9**, it is apparent that the ground state has a larger increase in the energy level relative to the corresponding transition state, as well as that the C=C bond length is correlated with the Gibbs free energy of activation, which decreases when the substituent at the stereogenic center becomes larger. It should be noted that there is a significant decrease in the energy barrier for the ^{t}Bu-substituted alkene **9c** as compared to the other smaller size substituents. The half-life at room temperature for alkene **4** was experimentally determined to be 3.17 min,[21] and a strong acceleration of the motor **9c** is expected if the activation energies for both alkenes are compared.

The overcrowded alkenes **9** were synthesized starting from the upper and lower half ketones **10** and **11** as building blocks (Scheme 1).

Scheme 1. Retro-synthesis of Alkenes **9**

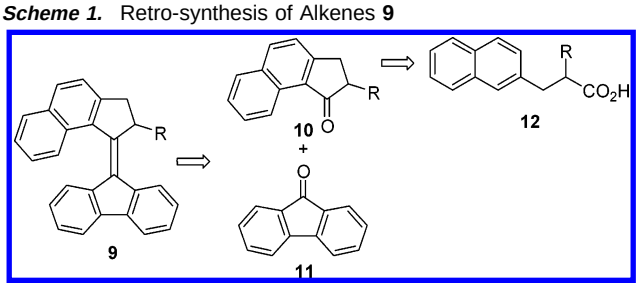

Ketones **10** were synthesized in good yields (67−75%) by means of a Friedel−Crafts cyclization of the acid chlorides derived from the carboxylic acids **12** (Scheme 2). Although three regioisomers are expected from the cyclization process if a phenyl substituent is present at the stereogenic center (**12a**) or two regioisomers if aliphatic substituents are present (**12b**,**d**), only the desired ketones **10** were obtained. The key step in the synthesis of alkenes **9** is the formation of the central olefinic bond. Attempts to generate the olefinic bond by reductive coupling of the ketones **10** and **11** using a cross McMurry reaction were unsuccessful with only homocoupling products isolated from the reaction mixture. Analogous to the synthesis of previously reported alkene **4**, the formation of the central double bond can be achieved via a Staudinger type diazo-thioketone coupling.[26] Accordingly, two opposite approaches can be taken: coupling between the diazo-compound **14** derived from the upper half and the thioketone **16** derived from the lower half or between the thioketone **15** derived from the upper half and the diazo-compound **17** (Scheme 3) derived from the lower half. The first of these approaches is preferred when an aryl substituent is present in the α-carbon (**10a**, R = Ph), because the attempts to synthesize the corresponding thioketone afforded mixtures of side products derived from the reaction of the stabilized thioenol tautomer (similar observations were reported by Lawesson when an α-proton is present in thioketone species[27]). Diazo-compound **14** was prepared by oxidation of the hydrazone **13** derived from the upper half ketone **10** with a hypervalent iodine reagent and used in situ for further steps (Scheme 2).[18]

With sterically more demanding aliphatic α-substituents (**10b**, R = ^{i}Pr; **10c**, R = ^{t}Bu), no reaction of ketones **10** with hydrazine was observed. Steric effects seem to be responsible for this lack of reactivity, which can be taken as an advantage for the stabilization of the corresponding thioketones **15**, given the excessive destabilization of the tetrasubstituted internal double bond expected in the cyclic thioenol tautomer. Accordingly, thioketones **15** were prepared cleanly in good yield (67−78%) by reaction of the corresponding ketones **10** with P_2S_5 with no trace of the undesirable thioenol (Scheme 2). Curiously, if an α-methyl substituent is present in the ketone **10**, both approaches can be taken. The synthesis of the alkene **4** (R = Me) was reported previously using a diazo-compound derived from the upper half (39%),[21] but higher yields (65%) can be achieved using the reverse coupling approach. A methyl moiety seems to be sufficiently large to destabilize the thioenol tautomer but small enough to allow the preparation of the hydrazone **13**.

Reaction of the diazo-compound **14a** derived from the phenyl-substituted upper half with fluorenethione **16** at low temperature

(26) ter Wiel, M. K. J.; Vicario, J.; Davey, S. G.; Meetsma, A.; Feringa, B. L. *Org. Biomol. Chem.* **2005**, *3*, 28.
(27) Scheibe, S.; Shabana, R.; Lawesson, S.-O. *Tetrahedron* **1982**, *38*, 993.

Scheme 2. Synthesis of the Diazo-Compounds **14** and Thioketones **15**[a]

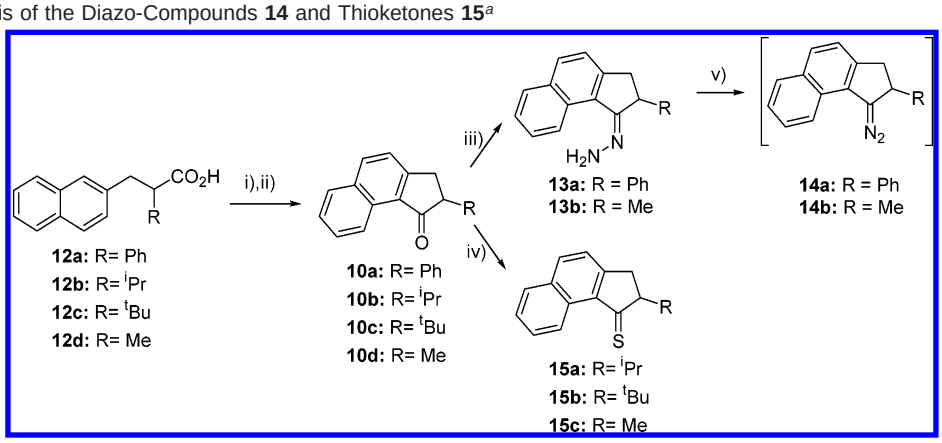

[a] Reagents and conditions: (i) $SOCl_2$, CH_2Cl_2, 40 °C; (ii) $AlCl_3$, CH_2Cl_2, 0 °C; (iii) H_2NNH_2, EtOH, 78 °C; (iv) P_2S_5, toluene, 111 °C; (v) bis(trifluoroacethoxy)iodobenzene, DMF, −30 °C.

Scheme 3. Synthesis of Overcrowded Alkenes[a]

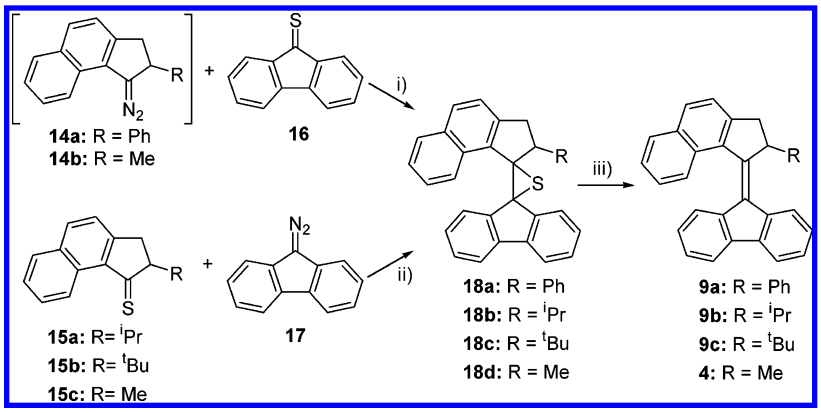

[a] Reagents and conditions: (i) DMF, −30 °C; (ii) toluene, 111 °C; (iii) PPh_3, toluene, 111 °C or xylene, 140 °C.

afforded a mixture of episulfide **18a** and alkene **9a** (1/1 ratio), which was treated directly with PPh_3 at high temperature to yield the alkene **9a** in moderate yield (36%) (Scheme 3). The same results were observed in the reaction between the alkyl-substituted thioketones **15a**−**c** derived from the upper half with diazofluorenone **17** in refluxing toluene, affording mixtures of episulfides **18b**−**d** and alkenes **9b**,**c** or **4**, which were treated in situ with PPh_3 to afford the corresponding alkenes **9b**,**c** or **4** in good yields (62−65%) (Scheme 3).

Alkenes **9** were fully characterized by ^1H and ^{13}C NMR spectroscopy and HRMS and X-ray analysis (for **9a** and **9c**). Comparison of the ^1H NMR chemical shifts as well as coupling constants for the diastereotopic CH_2 and the CH protons in the five-membered ring upper half for the aliphatic-substituted alkenes **9b**,**c** (see Experimental Section) with the values reported before for **4**[21] shows that they are consistent with a pseudoaxial orientation of the R substituent at the stereogenic center. The stable conformation was confirmed by the X-ray structure of compounds **9a** and **9c** (Figure 2). It was established that the (*R*)-enantiomer showed a preferred (*M*)-helicity, while the (*S*)-enantiomer showed a preferred (*P*)-helicity.

Other important features derived from the crystal structures of alkenes **9a** and **9c** are the nonplanar structure of the tetrasubstituted central alkene (Figure 2, projections) due to the overcrowded environment and the rigid lower half. The axial substituent at the stereogenic center points away from the olefinic bond to diminish the strain in the structure. The torsion angles on the olefinic bonds between the lower and upper half

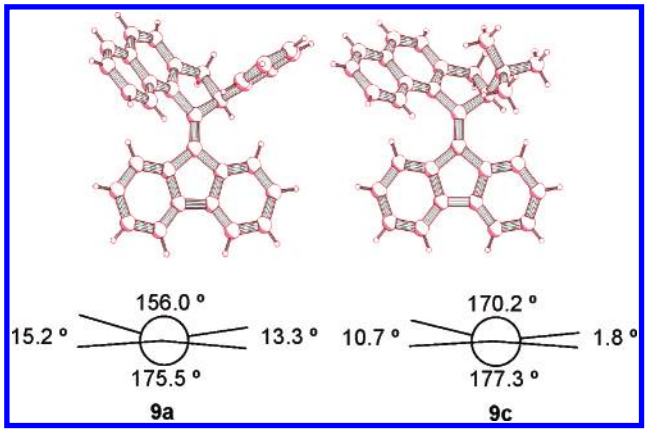

Figure 2. X-ray structure for alkenes **9a** and **9c** ((*S*)-enantiomer shown).

are 15.2° and 13.3° for **9a** and 10.7° and 1.8° for **9c**. The fluorene lower half is only 4.5° out of planarity in **9a** and 2.7° in **9c**, while the dihedral angles in the five-membered ring upper half are 156.0° in **9a** and 170.2° in **9c**. The helical shape of the molecule is evident from the angles between the fluorene lower half and the naphthalene upper half, 51.2° for **9a** and 54.8° for **9c** (Figure 2). It is clear that the double bond is considerably twisted in both cases. The larger ^{t}Bu substituent in **9c** pushes the naphthalene upper half further away from the fluorene lower half (pitch of the helix increases) as compared to the smaller Ph group in **9a**. As a consequence, the enhanced strain in **9c** relative to **9a** is reflected in a longer C═C distance (1.357 Å for **9a** and 1.387 Å for **9c**).

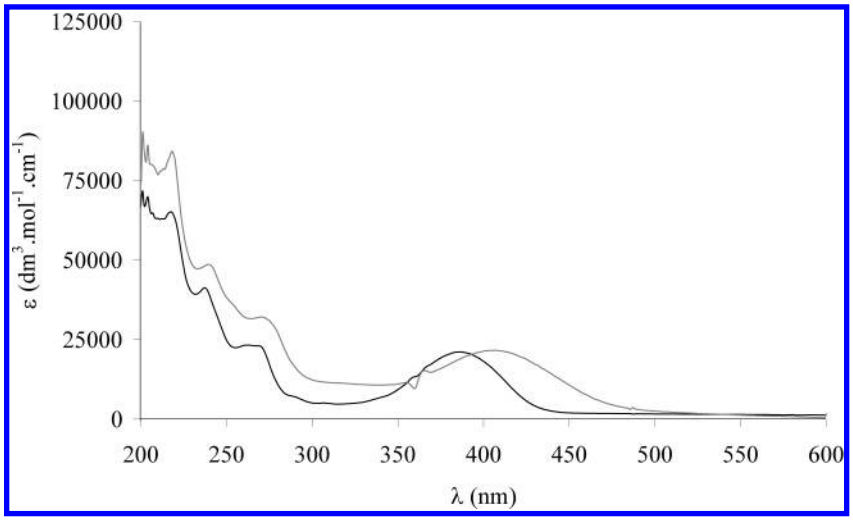

Figure 3. UV−vis spectra of **9a** at −20 °C in hexane before (black) and after irradiation (gray).

Scheme 4. Photochemical Cis/Trans Isomerization and Thermal Helix Inversion Steps of Alkenes **9** ((*S*)-Enantiomer Shown)

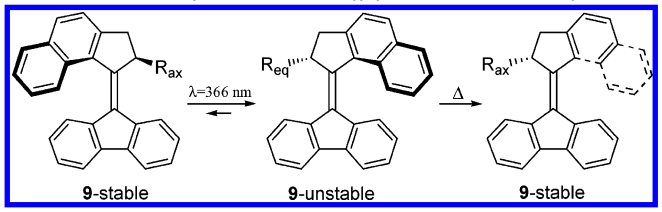

Table 2. ^{1}H NMR Shifts in Toluene-d_8 for the Proton in the Stereogenic Center and PSS_{365nm} for Alkenes **4** and **9**

alkene	R	δ_{CHeq} (ppm)	δ_{CHax} (ppm)	PSS (unst/st)[a]
4	Me	4.06	3.77	75/25
9a	Ph	5.20	4.41	86/14
9b	^{i}Pr	4.08	3.84	89/11
9c	^{t}Bu	4.35	4.07	88/12

[a] Determined by the integration of ^{1}H NMR peaks.

Photochemical experiments (λ = 366 ± 5 nm) were performed in hexane at −20 °C for the alkenes **9a** and **9b** or at −60 °C for the alkene **9c**. Upon irradiation of the alkenes **9**, cis/trans isomerization afforded a new isomer (denoted the unstable isomer), which was monitored by UV−vis spectroscopy as a shift of the absorption around 390 nm to a broader band at higher wavelength (**9a**, 392 to 415 nm; **9b**, 390 to 430 nm; and **9c**, 398 to 442 nm). This bathochromic shift is attributed to enhanced twist of the central olefinic bond.[19,20] Figure 3 shows representative UV−vis spectra for stable and unstable forms of alkene **9a**. Subsequent warming of the samples to room temperature resulted in identical UV−vis spectra as measured for the initial states, indicating thermal isomerization and regeneration of the stable isomers (Scheme 4).

To characterize the unstable intermediates, irradiation (λ = 366 ± 5 nm) of NMR samples was performed at −40 °C for the alkenes **9a** and **9b** and at −80 °C for the alkene **9c**, and the photochemical and thermal isomerization processes were monitored by ^{1}H NMR spectroscopy. Upon irradiation of a toluene-d_8 solution of alkenes **9**, an upfield shift of the signal corresponding to the proton at the stereogenic center was observed (Table 2), indicating a pseudoequatorial to pseudoaxial conformational change. As a consequence, the aromatic or aliphatic substituent at the stereogenic center adopts the less stable pseudoequatorial orientation (Scheme 4).

The ratio unstable/stable at the photostationary state was determined by the integration of the upper ring CH signal (Table 2). Warming the irradiated sample to room temperature resulted in a first-order thermal isomerization process, affording the stable isomers of **9a**−**c** with a pseudoaxial orientation of the R-substituent (Scheme 4). The ^{1}H NMR spectra of **9a** shown in Figure 4 before and after irradiation and after warming to room temperature are representative of the changes observed in the 180° rotation process in these systems.

Given that photochemical cis/trans isomerization and the thermal isomerization process both result in a helix inversion, CD spectroscopy is a convenient tool for monitoring the rotary cycle. Resolution of the alkenes **9** was achieved by chiral HPLC (Chiracel-OD column). Irradiation of a solution of enantiopure molecule **9a** in hexane at low temperature showed inversion of the major absorption bands in the CD spectrum, indicating photoisomerization and simultaneous helix inversion. Warming the sample to room temperature fully restored the CD spectrum of the initial state (Figure 5). Similar changes in CD spectra were observed for **9b** and **9c** (see Experimental Section).

After irradiation of the motor molecules **9**, the samples were heated and the change in the intensity of the maximum CD bands over time was measured at several temperatures. This allowed monitoring of the rate of conversion of the less stable isomers, and, therefore, the rate constant (k) for the first-order thermal helix inversion process at different temperatures was obtained. The enthalpy of activation ($\Delta H^{\ddagger}$) and entropy of activation ($\Delta S^{\ddagger}$) were determined from the rate constant by means of the Eyring plot, and from this the Gibbs free energy of activation ($\Delta^{\ddagger}G°$), the rate constant (k^0), and the half-life ($t_{1/2}$) at room temperature were calculated. The results are summarized in Table 3, including the values determined for the methyl-substituted molecular motor **4** previously reported.[21]

The calculated half-lives of the motor series indicate that an increase in the size of the substituents enhances the speed of rotation, suggesting that the initial state (unstable form) corresponding to the thermal helix inversion is raised in energy more than the corresponding transition state. As a consequence, the energy barrier is lowered as the size of the substituent is increased, which results in an acceleration of the thermal helix

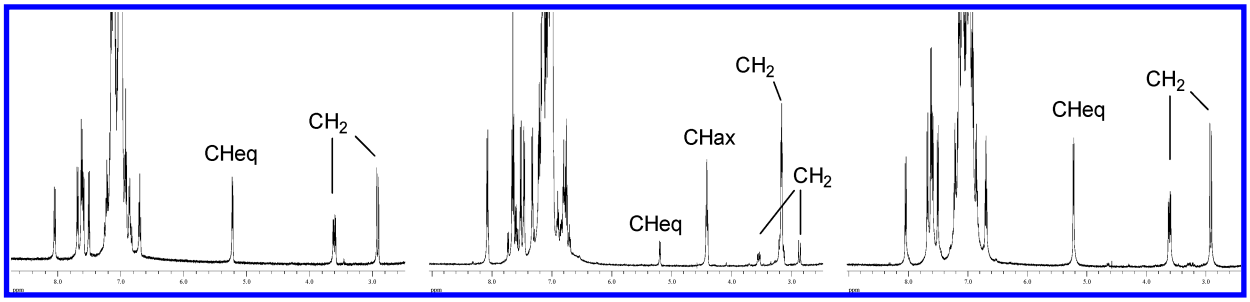

Figure 4. ^{1}H NMR in toluene-d_8 at −30 °C of **9a** before irradiation (left), after irradiation (center), and after being warmed to room temperature (right).

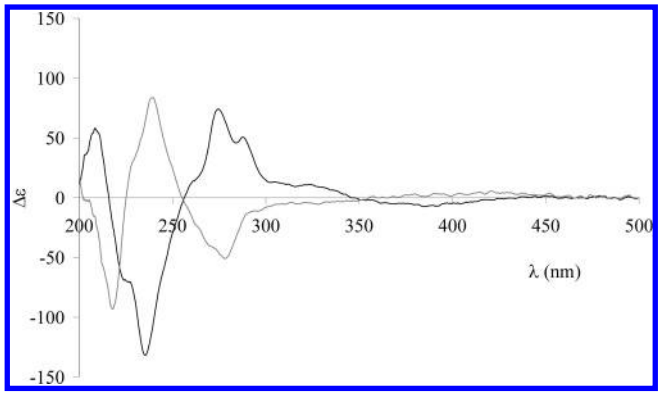

Figure 5. CD spectra of **9a** in hexane at −20 °C before (black) and after irradiation (gray).

Table 3. Thermodynamic Parameters for Molecular Motors **4** and **9**

motor	R	k^0 (s^{-1})	$\Delta^{\ddagger}G°$ (kJ mol^{-1})	$t_{1/2}$ (s)
9a	Ph	1.18×10^{-3}	88	587
4	Me	3.64×10^{-3}	85	190
9b	^{i}Pr	7.32×10^{-3}	84	95
9c	^{t}Bu	1.21×10^{2}	60	5.74×10^{-3}

inversion step. The order of magnitude of empirical data is in accordance with the calculated data for the alkenes **4** and **9a**−**c** (see Table 1), and the deviation is between 5% and 11%. The most remarkable finding is that the change of a Me group in **4** for a ^{t}Bu group in **9c** reduces the half-life by a factor of 30 000 and gives access to a light-driven molecular motor with at least one-half of the molecules with a frequency of 87 turns per second. Considering the thermal isomerization as the rate-limiting step, this speed of rotation has potential for future applications of these motors as molecular propellers.

However, another key question to be addressed is, if both photochemical cis/trans isomerization and thermal isomerization processes are unidirectional, is the energy barrier between the final state (stable form) and the transition state for the thermal isomerization still sufficiently high to be considered as an irreversible process? To demonstrate unequivocally the unidirectionality of the entire 360° rotary cycle for the fastest motor **9c**, molecular motor **20** with a nonsymmetrical fluorene lower half was synthesized from the upper half derived thioketone **15b** and 2-methoxy-9-diazo-fluorene **19** (Scheme 5). Alkene **20** was obtained as a cis/trans mixture (1:2 ratio), and *trans*-**20** and *cis*-**20** were separated by chromatography using a mixture of SiO_2/$AgNO_3$ 9/1 as stationary phase and were purified subsequently by repeated recrystallizations.

The calculated rate constant k at −85 °C for the ^{t}Bu-substituted alkene **9c** is 1.76×10^{-5} s^{-1}, and, analogously, for

Scheme 5. Synthesis of the Unsymmetrical Alkene **20**[a]

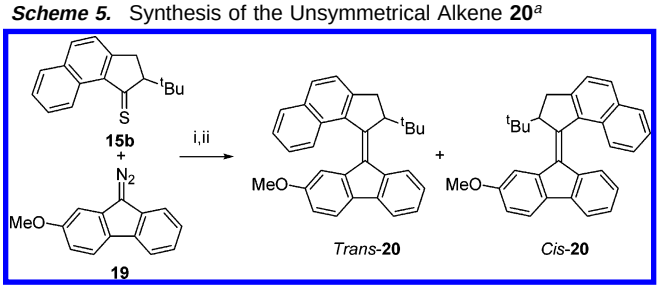

[a] Reagents and conditions: (i) toluene, 111 °C; (ii) PPh_3, xylene, 140 °C.

Scheme 6. 360° Rotary Cycle for the Nonsymmetrical Motor **20** As Observed by ^{1}H NMR (One Enantiomer Shown)

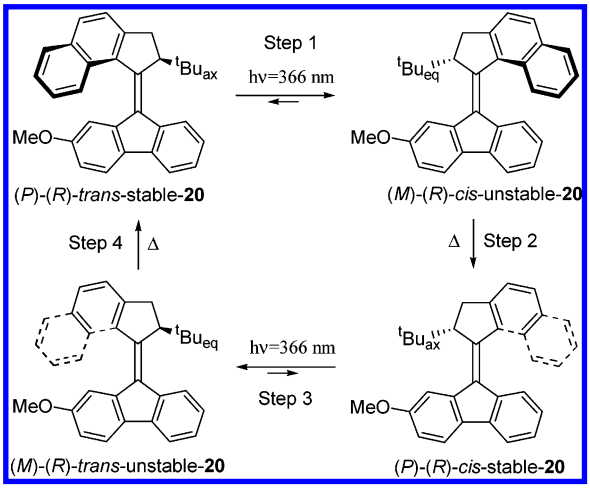

the unsymmetrical alkene **20** we expected that at low temperature in 48 min approximately 5% of the unstable form could undergo thermal isomerization. To avoid thermal isomerization and achieve the maximum ratio of cis/trans in the photochemical conversion, a dilute solution of pure *trans*-stable-**20** in toluene-d_8 was irradiated for 45 min at −85 °C. An upfield shift of the absorption corresponding to the CH at the stereogenic center was observed (4.35 to 4.09 ppm), indicating a pseudoaxial to pseudoequatorial conformational change of the ^{t}Bu group, as well as a downfield shift of the singlet corresponding to the methoxy group (2.62 to 3.38 ppm), which indicates a trans to cis conversion. A photoequilibrium comprising *cis*-unstable-**20**/*trans*-stable-**20** with a ratio 52/48 was determined by integration of signals for pseudoequatorial and pseudoaxial protons at the stereogenic center. No other possible *trans*-unstable or *cis*-stable isomers were observed. Heating of the sample to room temperature resulted exclusively in transformation of *cis*-unstable-**20** to *cis*-stable-**20** (Scheme 6), because the ratio *trans*-stable-**20**/*cis*-stable-**20**, determined by the integration of the methoxy singlets, is equivalent to the ratio *trans*-stable-

20/*cis*-unstable-**20** at the photoequilibrium. Thermal cis/trans isomerization can, therefore, be excluded, confirming theunidirectionality of the irreversible thermal isomerization of *cis*-unstable-**20**. Similar results were obtained when the irradiation of a diluted solution of pure *cis*-stable-**20** was carried out at −85 °C for 45 min. In this case, an upfield shift of the signal corresponding to the CH at the stereogenic center (4.33 to 4.05 ppm) as well as an upfield shift of the singlet corresponding to the methoxy group (3.54 to 2.67 ppm) were observed. This indicates a pseudoequatorial to pseudoaxial conformational change for the proton at the stereogenic center (or pseudoaxial to pseudoequatorial conformational change of the ^{t}Bu group) and cis to trans conversion. The photoequilibrium ratio *trans*-unstable-**20**/*cis*-stable-**20** was determined in this case to be 60/40. Heating of the irradiated sample showed the transformation of *trans*-unstable-**20** exclusively to *trans*-stable-**20** (Scheme 6), demonstrating the unidirectionality of the overall 360° rotary cycle. The combination of two photochemical isomerization steps (step 1, step 3, reversible) with two thermal unidirectional isomerization steps (step 2, step 4) ensures a full 360° rotary cycle of the upper propeller unit with respect to the lower fluorene unit.

Conclusions

A new family of second-generation light-driven molecular motors with different size substituents at the stereogenic center is described in this paper. The experimental data demonstrate that an increase of the size of the substituent at the stereogenic center speeds up the rotary motion as the thermal helix inversion barrier is lowered. This is in agreement with the theoretical calculations, which suggests that both steric and conformational aspects are involved in the thermal helix inversion step. The use of different substituents allows the tuning of the speed of rotation in a very convenient range of rotation frequencies for future applications. The slowest motors **9a**,**b** described here are under investigation as chiral dopants in liquid crystals, while applications of **9c**, the fastest light-driven unidirectional molecular motor reported thus far in the development of nanomachines propelled by molecular motors, currently are being explored.

Experimental Section

Irradiation experiments were performed with a Spectroline ENB-280C/FE UV lamp at 366 nm. Photostationary states were ensured monitoring composition changes in time by taking UV spectra at distinct intervals until no changes were observed using a Hewlet-Packard HP 8543 FT spectrophotometer. Thermal helix inversions were monitored by CD spectroscopy using a JASCO J-715 spectropolarimeter and a JASCO PFD-350S/350L Peltier-type FDCD attachment with temperature control. Uvasol-grade solvents (Merck) were used. NMR spectra were obtained using a Varian Mercury Plus and a Varian Unity Plus Varian-500, operating at 399.93 and 499.86 MHz, respectively, for the ^{1}H nucleus, or at 100.57 and 125.70 MHz, respectively, for the ^{13}C nucleus. Chemical shifts are reported in δ units (ppm) relative to the residual deuterated solvent signals of $CDCl_3$ (^{1}H NMR, δ 7.26 ppm; ^{13}C NMR, δ 77.0 ppm) or toluene-d_8 (^{1}H NMR, δ 2.09 ppm). Density functional theory (DFT) calculations were carried out with the Gaussian 03W (rev. C.02) program package.[28] All of the calculations were performed on systems in the gas phase using the Becke's three-parameter hybrid functional[29] with the LYP correlation functional[30] (B3LYP). The geometry optimization was followed by the frequency calculation to prove that the energy minimum or the transition state was found. For compounds with more conformations with minimum energy, the conformation with the lowest energy was chosen. Methyl (2-methyl-2,3-dihydro-cyclopenta[*a*]naphthalen-1-ylidene)-hydrazine was synthesized following the literature procedure.[26]

General Procedure for the Synthesis of Alkenes 9 and 4. Procedure A. To a stirred solution of fluorenone (0.540 g, 3 mmol) in toluene (9 mL) was added Lawesson's reagent (1.62 g, 4 mmol). The mixture was heated at 80 °C until a dark green color was observed (approx. 2 h) and then cooled under an atmosphere of nitrogen and poured onto a SiO_2 column. After rapid chromatography, using a mixture of hexane/CH_2Cl_2 9:1 as the eluent, the green solution from the column was directly added to a stirred solution of diazo-compound prepared by addition of bis(trifluoroacethoxy)iodobenzene (1.290 g, 3 mmol) to a solution of the corresponding hydrazone **13** (3 mmol) in DMF (9 mL) at −30 °C. The reaction mixture was allowed to warm to room temperature, and the solvents were removed under reduced pressure. The resulting oil was washed with a saturated aqueous solution of NH_4Cl (25 mL) and extracted with ether. The organic solution was washed with H_2O, dried over $MgSO_4$, and concentrated under reduced pressure. The crude mixture of episulfide **18** and alkene **9** was dissolved in xylene and stirred overnight under reflux with PPh_3 (1.57 g, 6 mmol). The resulting mixture was cooled to room temperature, and MeI (0.560 mL, 9 mmol) was added to remove the excess of PPh_3. After 1 h at room temperature, the suspension formed was filtered and the solution was concentrated under reduced pressure. The crude residue was purified by column chromatography (SiO_2, pentane:ether = 19:1). **Procedure B.** A solution of the corresponding diazafluorene **17** or **19** (2 mmol) and thioketone **15** (1 mmol) in toluene (5 mL) was stirred under reflux for 6 h. The resulting mixture of episulfide **18** and alkene **9** was treated with PPh_3 (0.524 g, 2 mmol) and stirred at reflux overnight. The reaction mixture was cooled to room temperature, and MeI (0.187 mL, 3 mmol) was added to remove the excess of PPh_3. The suspension obtained was filtered, and the solution was concentrated under reduced pressure. The crude residue was purified by column chromatography (SiO_2, pentane:ether = 19:1).

9-(2-Phenyl-2,3-dihydro-cyclopenta[*a*]naphthalen-1-ylidene)-9H-fluorene (9a). The general procedure A was followed, using (2-phenyl-2,3-dihydro-cyclopenta[*a*]naphthalen-1-ylidene)-hydrazine **13a** (0.816 g, 3 mmol), affording 0.441 g (36%) of the alkene **9a** as a yellow solid. ^{1}H NMR (400 MHz, $CDCl_3$): δ 3.21 (d, $^2J_{HH}$ = 15.0 Hz, 1H, CH_2), 3.98 (dd, $^2J_{HH}$ = 15.0 Hz, $^3J_{HH}$ = 6.6 Hz, 1H, CH_2), 5.37 (d, $^3J_{HH}$ = 6.6 Hz, 1H, CH), 6.80−6.88 (m, 2H), 7.11−7.27 (m, 7H), 7.31 (t, $^3J_{HH}$ = 7.7 Hz, 1H), 7.41−7.53 (m, 4H), 7.77 (d, $^3J_{HH}$ = 7.7 Hz, 1H), 7.80 (d, $^3J_{HH}$ = 7.7 Hz, 1H), 7.87 (d, $^3J_{HH}$ = 8.4 Hz, 1H), 7.94 (d, $^3J_{HH}$ = 8.1 Hz, 1H), 8.00 (d, $^3J_{HH}$ = 8.1 Hz, 1H). ^{13}C NMR (75 MHz, $CDCl_3$): δ 44.1 (CH_2), 56.5 (CH), 119.1 (CH), 119.5 (CH), 123.7 (CH), 124.4 (CH), 125.5 (CH), 125.8 (CH), 126.1 (CH), 126.4 (CH), 127.0 (2CH), 127.2 (3CH), 127.6 (CH), 128.7 (CH), 128.8 (CH), 129.0 (C), 131.1 (CH), 132.7 (C), 133.0 (C), 137.0 (C), 137.6 (C), 139.5 (C), 139.8 (C), 140.1 (C), 143.9 (C), 146.2 (C), 146.4 (C). *m*/*z* (EI, %) = 406 (M^+, 84), 328 (100), 273 (35), 241 (43), 196 (68), 165 (32). HRMS (EI): calcd for $C_{32}H_{22}$, 406.174; found, 406.172.

9-(2-Isopropyl-2,3-dihydro-cyclopenta[*a*]naphthalen-1-ylidene)-9H-fluorene (9b). The general procedure B was followed, using 2-isopropyl-2,3-dihydro-cyclopenta[*a*]naphthalen-1-one **15a** (0.240 g, 1 mmol) and 9-diazo-9H-fluorene **17** (0.384 g, 2 mmol), affording 0.441 g (62%) of the alkene **9b** as a yellow solid. ^{1}H NMR (400 MHz, $CDCl_3$): δ 0.61 (d, $^3J_{HH}$ = 7.0 Hz, 3H, CH_3), 1.18 (d, $^3J_{HH}$ = 7.0 Hz, 3H, CH_3), 2.30 (m, 1H, CH), 2.98 (d, $^2J_{HH}$ = 15.4 Hz, 1H, CH_2), 3.43 (dd, $^3J_{HH}$ = 5.5 Hz, $^2J_{HH}$ = 15.4 Hz, 1H, CH_2), 4.24 (d, $^3J_{HH}$ = 5.5 Hz,

(28) Frisch, M. J.; et al. *Gaussian 03*, revision C.02; Gaussian, Inc.: Wallingford, CT, 2004.

(29) Becke, A. D. *J. Chem. Phys.* **1993**, *98*, 5648.
(30) Lee, C.; Yang, W.; Parr, R. G. *Phys. Rev.* **1988**, *B37*, 785.

1H, CH), 6.74 (d, $^3J_{HH}$ = 8.1 Hz, 1H), 6.80 (t, $^3J_{HH}$ = 7.7 Hz, 1H), 7.23 (t, $^3J_{HH}$ = 7.7 Hz, 1H), 7.34 (t, $^3J_{HH}$ = 8.1 Hz, 1H), 7.41 (d, $^3J_{HH}$ = 5.9 Hz, 1H), 7.42 (d, $^3J_{HH}$ = 5.5 Hz, 1H), 7.47 (d, $^3J_{HH}$ = 8.1 Hz, 1H), 7.55 (d, $^3J_{HH}$ = 8.4 Hz, 1H), 7.77 (d, $^3J_{HH}$ = 7.7 Hz, 1H), 7.79 (d, $^3J_{HH}$ = 7.7 Hz, 1H), 7.87 (dd, $^3J_{HH}$ = 3.3, $^3J_{HH}$ = 5.8 Hz, 1H), 7.89 (d, $^3J_{HH}$ = 8.1 Hz, 1H), 7.94 (d, $^3J_{HH}$ = 8.4 Hz, 1H), 8.03 (dd, $^3J_{HH}$ = 3.3, $^3J_{HH}$ = 5.5 Hz, 1H). ^{13}C NMR (75 MHz, $CDCl_3$): δ 18.5 (CH_3), 20.9 (CH_3), 31.2 (CH), 36.2 (CH_2), 56.3 (CH), 118.8 (CH), 119.6 (CH), 123.2 (CH), 124.2 (CH), 125.2 (CH), 125.8 (CH), 125.9 (CH), 126.6 (CH), 126.7 (CH), 126.8 (CH), 126.9 (CH), 127.3 (CH), 128.6 (CH), 129.1 (C), 130.7 (CH), 131.0 (C), 132.4 (C), 137.1 (C), 137.9 (C), 139.3 (C), 139.7 (C), 140.3 (C), 148.2 (C), 150.4 (C). *m*/*z* (EI, %) = 372 (M^+, 46), 329 (100). HRMS (EI): calcd for $C_{29}H_{24}$, 372.186; found, 372.188.

9-(2-*tert*-Butyl-2,3-dihydro-cyclopenta[*a*]naphthalen-1-ylidene)-9H-fluorene (9c). The general procedure B was followed, using 2-*tert*-butyl-2,3-dihydro-cyclopenta[*a*]naphthalen-1-thione **15b** (0.254 g, 1 mmol) and 9-diazo-9H-fluorene **17** (0.384 g, 2 mmol), affording 0.251 g (65%) of the alkene **9c** as a yellow solid. ^{1}H NMR (400 MHz, $CDCl_3$): δ 0.87 (s, 9H, CH_3), 3.02 (d, $^2J_{HH}$ = 15.0 Hz, 1H, CH_2), 3.41 (dd, $^3J_{HH}$ = 5.5 Hz, $^2J_{HH}$ = 15.0 Hz, 1H, CH_2), 4.56 (d, $^3J_{HH}$ = 5.5, 1H, CH), 6.70−6.76 (m, 2H), 7.21 (t, $^3J_{HH}$ = 7.3 Hz, 1H), 7.34 (t, $^3J_{HH}$ = 8.1 Hz, 1H), 7.39−7.42 (m, 2H), 7.46 (t, $^3J_{HH}$ = 8.1 Hz, 1H), 7.54 (t, $^3J_{HH}$ = 8.4 Hz, 1H), 7.75−7.77 (m, 2H), 7.86 (dd, $^3J_{HH}$ = 3.7, $^3J_{HH}$ = 7.0 Hz, 1H), 7.89 (d, $^3J_{HH}$ = 8.1 Hz, 1H), 7.94 (d, $^3J_{HH}$ = 8.1 Hz, 1H), 8.35 (dd, $^3J_{HH}$ = 3.7, $^3J_{HH}$ = 7.0 Hz, 1H). ^{13}C NMR (75 MHz, $CDCl_3$): δ 28.7 (CH_3), 35.9 (C), 37.3 (CH_2), 59.5 (CH), 118.6 (CH), 119.5 (CH), 123.0 (CH), 125.1 (CH), 125.2 (CH), 125.8 (CH), 126.0 (CH), 126.2 (CH), 126.6 (CH), 126.8 (CH), 126.9 (CH), 127.0 (CH), 128.7 (CH), 129.1 (C), 130.4 (CH), 131.1 (C), 132.1 (C), 137.3 (C), 139.1 (C), 139.3 (C), 139.6 (C), 140.7 (C), 147.6 (C), 149.8 (C). *m*/*z* (EI, %) = 386 (M^+, 31), 329 (100). HRMS (EI): calcd for $C_{30}H_{26}$, 386.203; found, 386.203.

9-(2-Methyl-2,3-dihydro-cyclopenta[*a*]naphthalen-1-ylidene)-9H-fluorene (4). The general procedure A was reported with 39% yield.[21] Procedure B was followed, using 2-methyl-2,3-dihydro-cyclopenta[*a*]-naphthalene-1-thione **15c** (0.212 g, 1 mmol) and 9-diazafluorene **17** (0.384 g, 2 mmol), affording 0.441 g (65%) of alkene **4** as a yellow solid. Spetroscopic data are in agreement with literature values.

***trans*-9-(2-*tert*-Butyl-2,3-dihydro-cyclopenta[*a*]naphthalen-1-ylidene)-2-methoxy-9H-fluorene (*trans*-20).** The general procedure B was followed, using 2-*tert*-butyl-2,3-dihydro-cyclopenta[*a*]naphthalen-1-thione **15b** (0.254 g, 1 mmol) and 2-methoxy-9-diazafluorene **19** (0.444 g, 2 mmol), affording 0.262 (63%) of a mixture *cis*/*trans*-**20** (1:2 ratio) as a yellow solid. Separation of the isomers was carried out by column chromatography (SiO_2/$AgNO_3$ 9:1, pentane/Et_2O 95:5), and 61 mg of pure *trans*-**20** was obtained after two consecutive crystallizations from heptane. ^{1}H NMR (400 MHz, $CDCl_3$): δ 0.89 (s, 9H, CH_3), 2.82 (s, 3H, OCH_3), 3.03 (d, $^2J_{HH}$ = 15.4 Hz, 1H, CH_2), 3.41 (dd, $^3J_{HH}$ = 5.5 Hz, $^2J_{HH}$ = 15.4 Hz, 1H, CH_2), 4.45 (d, $^3J_{HH}$ = 5.5, 1H, CH), 6.29 (d, $^4J_{HH}$ = 2.2 Hz, 1H), 6.77 (dd, $^4J_{HH}$ = 2.2 Hz, $^3J_{HH}$ = 8.4 Hz, 1H), 7.27−7.47 (m, 4H), 7.55 (d, $^3J_{HH}$ = 8.1 Hz, 1H), 7.60 (d, $^3J_{HH}$ = 8.4 Hz, 1H), 7.73 (d, $^3J_{HH}$ = 7.3 Hz, 1H), 7.80 (d, $^3J_{HH}$ = 8.1 Hz, 1H), 7.87 (d, $^3J_{HH}$ = 8.1 Hz, 1H), 7.92 (d, $^3J_{HH}$ = 8.1 Hz, 1H), 8.27 (d, $^3J_{HH}$ = 7.7 Hz, 1H). ^{13}C NMR (75 MHz, $CDCl_3$): δ 28.7 (CH_3), 35.9 (C), 37.3 (CH_2), 54.6 (OCH_3), 59.5 (CH), 109.9 (CH), 115.4 (CH), 118.8 (CH), 119.4 (CH), 123.1 (CH), 125.0 (CH), 125.1 (CH), 125.2 (CH), 126.8 (CH), 127.0 (CH), 127.3 (CH), 128.7 (CH), 129.0 (C), 130.4 (CH), 131.4 (C), 132.1 (C), 132.5 (C), 138.6 (C), 139.0 (C), 139.3 (C), 140.8 (C), 147.6 (C), 149.7 (C), 158.2 (C). *m*/*z* (EI, %) = 416 (M^+, 25), 359 (100). HRMS (EI): calcd for $C_{31}H_{28}O$, 416.214; found, 416.215.

***cis*-9-(2-*tert*-Butyl-2,3-dihydro-cyclopenta[*a*]naphthalen-1-ylidene)-2-methoxy-9H-fluorene (*cis*-20).** Following separation of the isomers by column chromatography (SiO_2/$AgNO_3$ 9:1, pentane/Et_2O 95:5), 29 mg of pure *cis*-**20** was obtained after three consecutive crystallizations from heptane. ^{1}H NMR (400 MHz, $CDCl_3$): δ 0.87 (s, 9H, CH_3), 3.00 (d, $^2J_{HH}$ = 15.0 Hz, 1H, CH_2), 3.37 (dd, $^3J_{HH}$ = 5.5 Hz, $^2J_{HH}$ = 15.0 Hz, 1H, CH_2), 3.97 (s, 3H, OCH_3), 4.39 (d, $^3J_{HH}$ = 5.5, 1H, CH), 6.62−6.66 (m, 2H), 6.96 (dd, $^4J_{HH}$ = 2.2 Hz, $^3J_{HH}$ = 8.4 Hz, 1H), 7.15 (m, 1H), 7.34 (dd, $^3J_{HH}$ = 7.3 Hz, $^3J_{HH}$ = 7.7 Hz, 1H), 7.46 (dd, $^3J_{HH}$ = 7.7 Hz, $^3J_{HH}$ = 7.7 Hz, 1H), 7.53 (d, $^3J_{HH}$ = 7.7 Hz, 1H), 7.63 (d, $^3J_{HH}$ = 7.7 Hz, 1H), 7.72 (d, $^3J_{HH}$ = 8.4 Hz, 1H), 7.75 (d, $^3J_{HH}$ = 8.1 Hz, 1H), 7.87−7.90 (m, 2H), 7.93 (d, $^3J_{HH}$ = 7.7 Hz, 1H). ^{13}C NMR (75 MHz, $CDCl_3$): δ 28.8 (CH_3), 35.8 (C), 37.4 (CH_2), 55.7 (OCH_3), 59.7 (CH), 111.5 (CH), 112.6 (CH), 117.9 (CH), 120.0 (CH), 123.0 (CH), 124.8 (CH), 125.2 (CH), 125.9 (CH), 126.6 (CH), 127.0 (CH), 127.1 (CH), 128.7 (CH), 129.1 (C), 130.4 (CH), 132.1 (C), 134.2 (C), 137.1 (C), 139.1 (C), 139.4 (C), 141.1 (C), 147.5 (C), 149.8 (C), 149.9 (C), 158.7 (C). *m*/*z* (EI, %) = 416 (M^+, 25), 359 (100). HRMS (EI): calcd for $C_{31}H_{28}O$, 416.214; found, 416.215.

UV Monitoring of the Rotary Cycle. A UV−vis spectrum of a solution of **9a** (2.31×10^{-6} M) or **9b** (a 2.15×10^{-6} M) at −20 °C or **9c** (1.78×10^{-6} M) at −60 °C in hexane was taken before and after irradiation, showing a shift in the absorption in the region 390−400 nm to 425−440 nm and indicating formation of the less stable isomer. Warming of the samples resulted in the same UV−vis spectra as before irradiation, indicating thermal isomerization. λ_{max} (ϵ): **9a$_{st}$**, 392 (20.500); **9a$_{unst}$**, 415 (17.900); **9b$_{st}$**, 390 (21.300); **9b$_{unst}$**, 430 (18.100); **9c$_{st}$**, 398 (20.800); **9c$_{unst}$**, 442 (18.300) nm (see Figure 3 for representative spectra of **9a** and Supporting Information for spectra of **9b** and **9c**).

CD Monitoring of the Rotary Cycle. A molar CD spectrum of an enantiopure solution of **9a** (7.32×10^{-6} M) or **9b** (a 8.01×10^{-6} M) at −20 °C or **9c** (9.04×10^{-6} M) at −60 °C in hexane was taken before and after 10 min irradiation, showing in all cases complete inversion of the CD spectra and indicating the formation of the unstable isomer by cis/trans isomerization. Warming of the samples to room temperature showed again inversion of the CD signal to the original spectra, indicating formation of the stable isomer by thermal isomerization. λ_{max} ($\Delta\epsilon$): **9a$_{st}$**, 235 (−133.3), 276 (+73.0), 286 (+50.1); **9a$_{unst}$**, 237 (+80.6), 275 (−47.8); **9b$_{st}$**, 235 (−118.6), 270 (+88.0); **9b$_{unst}$**, 238 (+76.4), 280 (−65.3); **9c$_{st}$**, 235 (−118), 269 (+103.8), 287 (+94.4); **9c$_{unst}$**, 242 (−85.2), 261 (−65.1), 286 (−59.2) nm (see Figure 4 for representative spectra of **9a** and Supporting Information for spectra of **9b** and **9c**).

^{1}H NMR Monitoring of the Rotary Cycle. Irradiation (366 ± 5 nm) of a solution of **9a** or **9b** at −40 °C, **9c** at −60 °C, or *cis*-**20** and *trans*-**20** at −85 °C in toluene-d_8 was performed in a MeOH bath. ^{1}H NMR spectra of the samples before and after irradiation were taken at the same temperature as during the irradiation experiment, showing a completely different spectrum and indicating formation of the unstable isomer. Upon warming of the samples to room temperature only the stable isomer could be observed by ^{1}H NMR.

9a$_{st}$. ^{1}H NMR (500 MHz, toluene-d_8): δ 2.87 (d, $^2J_{HH}$ = 15.2 Hz, 1H, CH_2), 3.57 (dd, $^3J_{HH}$ = 6.6 Hz, $^2J_{HH}$ = 15.2 Hz, 1H, CH_2), 5.20 (d, $^3J_{HH}$ = 6.6 Hz, 1H, CH), 6.66 (dd, $^3J_{HH}$ = 7.2 Hz, $^3J_{HH}$ = 7.8 Hz, 1H), 6.83 (d, $^3J_{HH}$ = 6,9 Hz, 1H), 6.88 (dd, $^3J_{HH}$ = 7.5 Hz, $^3J_{HH}$ = 7.8 Hz, 1H), 6.95−7.15 (m, 9H overlapped with toluene), 7.19 (dd, $^3J_{HH}$ = 6.9 Hz, $^3J_{HH}$ = 7.8 Hz, 1H), 7.47 (d, $^3J_{HH}$ = 8.1 Hz, 1H), 7.56−7.60 (m, 3H), 7.65 (d, $^3J_{HH}$ = 7.8 Hz, 1H), 8.01 (d, $^3J_{HH}$ = 8.4 Hz, 1H).

9a$_{unst}$. ^{1}H NMR (500 MHz, toluene-d_8): δ 3.09−3.21 (m, 2H, CH_2), 4.39 (dd, $^3J_{HH}$ = 7.3 Hz, $^3J_{HH}$ = 7.7 Hz, 1H, CH), 6.72 (dd, $^3J_{HH}$ = 7.3 Hz, $^3J_{HH}$ = 7.6 Hz, 1H), 6.76 (dd, $^3J_{HH}$ = 6.0 Hz, $^3J_{HH}$ = 7.3 Hz, 1H), 6.95−7.15 (m, 10H overlapped with toluene), 7.18 (dd, $^3J_{HH}$ = 7.3 Hz, $^3J_{HH}$ = 7.6 Hz, 1H), 7.29 (d, $^3J_{HH}$ = 6.0 Hz, 1H), 7.42 (d, $^3J_{HH}$ = 7.6 Hz, 1H), 7.19 (d, $^3J_{HH}$ = 7.6 Hz, 1H), 7.61 (d, $^3J_{HH}$ = 6.0 Hz, 1H), 7.62 (d, $^3J_{HH}$ = 8.3 Hz, 1H), 8.04 (d, $^3J_{HH}$ = 8.3 Hz, 1H).

9b$_{st}$. ^{1}H NMR (500 MHz, toluene-d_8): δ 0.38 (d, $^3J_{HH}$ = 6.6 Hz, 3H, CH_3), 0.95 (d, $^3J_{HH}$ = 6.6 Hz, 3H, CH_3), 2.21 (m, 1H, CH), 2.58 (d, $^2J_{HH}$ = 15.3 Hz, 1H, CH_2), 3.02 (dd, $^3J_{HH}$ = 5.6 Hz, $^2J_{HH}$ = 15.3 Hz, 1H, CH_2), 4.08 (dd, $^3J_{HH}$ = 4.2 Hz, $^3J_{HH}$ = 5.6 Hz, 1H, CH), 6.66 (dd, $^3J_{HH}$ = 7.0 Hz, $^3J_{HH}$ = 8.4 Hz, 1H), 6.93−7.16 (m, 3H overlapped

with toluene), 7.20 (dd, $^3J_{HH}$ = 7.0 Hz, $^3J_{HH}$ = 8.4 Hz, 1H), 7.23 (d, $^3J_{HH}$ = 8.4 Hz, 1H), 7.30 (dd, $^3J_{HH}$ = 7.0 Hz, $^3J_{HH}$ = 8.4 Hz, 1H), 7.36 (dd, $^3J_{HH}$ = 7.0 Hz, $^3J_{HH}$ = 8.4 Hz, 1H), 7.59 (d, $^3J_{HH}$ = 7.0 Hz, 1H), 7.60 (d, $^3J_{HH}$ = 8.4 Hz, 1H), 7.63 (d, $^3J_{HH}$ = 8.4 Hz, 1H), 7.68 (d, $^3J_{HH}$ = 8.4 Hz, 1H), 7.89 (d, $^3J_{HH}$ = 8.4 Hz, 1H), 8.08 (d, $^3J_{HH}$ = 7.0 Hz, 1H).

9b$_{unst}$. ^{1}H NMR (500 MHz, toluene-d_8): δ 0.40 (d, $^3J_{HH}$ = 6.7 Hz, 3H, CH_3), 0.86 (d, $^3J_{HH}$ = 6.7 Hz, 3H, CH_3), 2.77 (dd, $^3J_{HH}$ = 8.3 Hz, $^2J_{HH}$ = 18.0 Hz, 1H, CH_2), 2.93 (m, 1H, CH), 2.98 (d, $^2J_{HH}$ = 18.0 Hz, 1H, CH_2), 3.84 (dd, $^3J_{HH}$ = 3.7 Hz, $^3J_{HH}$ = 4.7 Hz, 1H, CH), 6.72 (dd, $^3J_{HH}$ = 7.4 Hz, $^3J_{HH}$ = 7.7 Hz, 1H), 6.92 (d, $^3J_{HH}$ = 8.0 Hz, 1H), 6.96 (dd, $^3J_{HH}$ = 7.4 Hz, $^3J_{HH}$ = 8.0 Hz, 1H), 6.93−7.16 (m, 2H overlapped with toluene), 7.18 (dd, $^3J_{HH}$ = 7.4 Hz, $^3J_{HH}$ = 7.7 Hz, 1H), 7.19 (d, $^3J_{HH}$ = 8.0 Hz, 1H), 7.21 (d, $^3J_{HH}$ = 7.3 Hz, 1H), 7.31 (dd, $^3J_{HH}$ = 7.4 Hz, $^3J_{HH}$ = 7.7 Hz, 1H), 7.60−7.62 (m, 2H), 7.67 (d, $^3J_{HH}$ = 7.4 Hz, 1H), 7.83 (d, $^3J_{HH}$ = 7.7 Hz, 1H), 7.99 (d, $^3J_{HH}$ = 8.4 Hz, 1H).

9c$_{st}$. ^{1}H NMR (500 MHz, toluene-d_8): δ 0.77 (s, 9H, CH_3), 2.67 (d, $^2J_{HH}$ = 15.3 Hz, 1H, CH_2), 3.09 (dd, $^3J_{HH}$ = 5.5 Hz, $^2J_{HH}$ = 15.3 Hz, 1H, CH_2), 4.35 (d, $^3J_{HH}$ = 5.5 Hz, 1H, CH), 6.59 (dd, $^3J_{HH}$ = 7.3 Hz, $^3J_{HH}$ = 8.0 Hz, 1H), 6.94 (d, $^3J_{HH}$ = 8.0 Hz, 1H), 6.95−7.16 (m, 2H overlapped with toluene), 7.18−7.30 (m, 4H), 7.55 (d, $^3J_{HH}$ = 7.3 Hz, 1H), 7.59 (d, $^3J_{HH}$ = 8.0 Hz, 1H), 7.65 (d, $^3J_{HH}$ = 8.0 Hz, 2H), 7.81 (d, $^3J_{HH}$ = 8.3 Hz, 1H), 8.37 (d, $^3J_{HH}$ = 7.6 Hz, 1H).

9c$_{unst}$. ^{1}H NMR (500 MHz, toluene-d_8): δ 0.70 (s, 9H, CH_3), 2.90 (broad d, $^2J_{HH}$ = 11.2 Hz, 1H, CH_2), 3.15 (broad d, $^2J_{HH}$ = 11.2 Hz, 1H, CH_2), 4.06 (broad s, 1H, CH), 6.76 (dd, $^3J_{HH}$ = 6.6 Hz, $^3J_{HH}$ = 7.9 Hz, 1H), 6.92 (dd, $^3J_{HH}$ = 6.6 Hz, $^3J_{HH}$ = 7.9 Hz, 1H), 6.93−7.16 (m, 6H overlapped with toluene), 7.47 (d, $^3J_{HH}$ = 7.9 Hz, 1H), 7.51 (d, $^3J_{HH}$ = 7.9 Hz, 1H), 7.53 (d, $^3J_{HH}$ = 7.9 Hz, 1H), 7.55 (d, $^3J_{HH}$ = 7.9 Hz, 1H), 7.88 (d, $^3J_{HH}$ = 8.0 Hz, 1H), 8.05 (d, $^3J_{HH}$ = 8.4 Hz, 1H).

***trans*-20$_{st}$.** ^{1}H NMR (500 MHz, toluene-d_8): δ 0.76 (s, 9H, CH_3), 2.61 (d, $^2J_{HH}$ = 15.1 Hz, 1H, CH_2), 2.62 (s, 3H, OCH_3), 3.04 (dd, $^3J_{HH}$ = 5.4 Hz, $^2J_{HH}$ = 15.1 Hz, 1H, CH_2), 4.35 (d, $^3J_{HH}$ = 5.4 Hz, 1H, CH), 6.54 (d, $^4J_{HH}$ = 2.2 Hz, 1H), 6.91 (dd, $^4J_{HH}$ = 2.2 Hz, $^3J_{HH}$ = 8.3 Hz, 1H), 6.97−7.16 (m, 4H overlapped with toluene), 7.22 (d, $^3J_{HH}$ = 8.3 Hz, 1H), 7.27 (dd, $^3J_{HH}$ = 3.1 Hz, $^3J_{HH}$ = 5.7 Hz, 1H), 7.55−7.59 (m, 3H), 7.83 (d, $^3J_{HH}$ = 8.3 Hz, 1H), 8.38 (dd, $^3J_{HH}$ = 3.1 Hz, $^3J_{HH}$ = 5.7 Hz, 1H).

***cis*-20$_{unst}$.** ^{1}H NMR (500 MHz, toluene-d_8): δ 0.77 (s, 9H, CH_3), 2.51 (dd, $^3J_{HH}$ = 5.4 Hz, $^2J_{HH}$ = 15.3 Hz, 1H, CH_2), 2.95 (d, $^2J_{HH}$ = 15.3 Hz, 1H, CH_2), 3.38 (s, 3H, OCH_3), 4.09 (d, $^3J_{HH}$ = 5.4 Hz, 1H, CH), 6.79 (dd, $^3J_{HH}$ = 7.4 Hz, $^3J_{HH}$ = 7.4 Hz, 1H), 6.84 (broad s, 1H), 6.90−7.30 (m, 6H overlapped with toluene), 7.32 (broad s, 2H), 7.57 (broad s, 1H), 7.97 (broad s, 1H), 8.45 (broad s, 1H).

***cis*-20$_{st}$.** ^{1}H NMR (500 MHz, toluene-d_8): δ 0.77 (s, 9H, CH_3), 2.60 (d, $^2J_{HH}$ = 15.0 Hz, 1H, CH_2), 3.05 (dd, $^3J_{HH}$ = 5.4 Hz, $^2J_{HH}$ = 15.0 Hz, 1H, CH_2), 3.54 (s, 3H, OCH_3), 4.33 (d, $^3J_{HH}$ = 5.4, 1H, CH), 6.57 (dd, $^3J_{HH}$ = 7.5 Hz, $^3J_{HH}$ = 7.5 Hz, 1H), 6.84 (dd, $^4J_{HH}$ = 1.8 Hz, $^3J_{HH}$ = 8.4 Hz, 1H), 6.54 (broad s, 1H), 6.89−7.17 (m, 3H overlapped with toluene), 7.21 (dd, $^3J_{HH}$ = 8.2 Hz, $^3J_{HH}$ = 7.6 Hz, 1H), 7.52 (d, $^3J_{HH}$ = 7.6 Hz, 1H), 7.56 (d, $^3J_{HH}$ = 8.2 Hz, 1H), 7.59 (d, $^3J_{HH}$ = 8.2 Hz, 1H), 7.63 (d, $^3J_{HH}$ = 8.2 Hz, 1H), 7.87 (d, $^3J_{HH}$ = 8.4 Hz, 1H), 8.04 (d, $^4J_{HH}$ = 1.8 Hz, 1H).

***trans*-8$_{unst}$.** ^{1}H NMR (500 MHz, toluene-d_8): δ 0.78 (s, 9H, CH_3), 2.67 (s, 3H, OCH_3), 2.82 (dd, $^3J_{HH}$ = 5.4 Hz, $^2J_{HH}$ = 15.4 Hz, 1H, CH_2), 3.04 (d, $^2J_{HH}$ = 15.4 Hz, 1H, CH_2), 4.05 (d, $^3J_{HH}$ = 5.4 Hz, 1H, CH), 6.58 (s, 1H), 6.86 (dd, $^3J_{HH}$ = 8.4 Hz, $^3J_{HH}$ = 7.7 Hz, 1H), 6.98−7.24 (m, 5H overlapped with toluene), 7.28 (dd, $^3J_{HH}$ = 7.0 Hz, $^3J_{HH}$ = 7.7 Hz, 1H), 7.45 (d, $^3J_{HH}$ = 8.3, 1H, CH), 7.52 (d, $^3J_{HH}$ = 7.7 Hz, 1H, CH), 7.56 (dd, $^3J_{HH}$ = 7.0 Hz, $^3J_{HH}$ = 7.7 Hz, 1H), 7.71 (d, $^3J_{HH}$ = 7.0, 1H, CH), 8.04 (dd, $^3J_{HH}$ = 7.7 Hz, $^3J_{HH}$ = 8.3 Hz, 1H).

Acknowledgment. Financial support from The Netherlands Organization for Scientific Research (NWO-CW), the Materials Science Centre, and the University of Groningen is acknowledged. J.V. thanks the Departamento de Educación, Universidades e Investigación del Gobierno Vasco, for a postdoctoral fellowship.

Supporting Information Available: Full experimental procedures and characterization data for hydrazone **13a** and thioketones **15a**−**c** and their intermediates, and UV−vis, CD, and ^{1}H NMR spectra of stable and unstable isomers of **9a**−**c** and **20**. This material is available free of charge via the Internet at http://pubs.acs.org.

JA058303M